

Synthesis of a Series of Rhodium Complexes, $\text{Tp}^{\text{iPr}}\text{Rh}^{\text{I}}\text{L}_2$ and $\text{Tp}^{\text{iPr}}\text{Rh}^{\text{III}}(\text{X})(\text{Y})(\text{MeCN})$, with the Hydridotris(3,5-diisopropylpyrazolyl)borato Ligand (Tp^{iPr}) from a Versatile Precursor, $(\kappa^3\text{-Tp}^{\text{iPr}})\text{Rh}(\text{coe})(\text{MeCN})$, and Dependence of $\kappa^2\text{-}\kappa^3$ Interconversion Rate of the Tp^{iPr} Ligand on the Chelate Ring Size

Keisuke Ohta, Mariko Hashimoto, Yoshiaki Takahashi, Shiro Hikichi, Munetaka Akita,* and Yoshihiko Moro-oka*

Research Laboratory of Resources Utilization, Tokyo Institute of Technology, 4259 Nagatsuta, Midori-ku, Yokohama 226-8503, Japan

Received February 17, 1999

The labile Rh(I) species $\text{Tp}^{\text{iPr}}\text{Rh}(\text{coe})(\text{MeCN})$ (**1**) was prepared by the reaction of $[\text{RhCl}(\text{coe})_2]_2$ with KTp^{iPr} followed by crystallization from MeCN. Subsequent treatment of **1** with diphosphines and CO gave square-planar $\text{Tp}^{\text{iPr}}\text{RhL}_2$ -type products via replacement of the coe and MeCN ligands. The Rh(III) complexes $\text{Tp}^{\text{iPr}}\text{Rh}(\text{X})(\text{Y})(\text{MeCN})$ were obtained via oxidative addition of XY and dissociation of the coe ligand. Complex **1** serves as a versatile starting compound for a variety of Rh(I) and Rh(III) complexes containing the Tp^{iPr} ligand. In addition, it was found that $\kappa^2\text{-}\kappa^3$ interconversion of the diphosphine complexes $\text{Tp}^{\text{iPr}}\text{Rh}[\text{Ph}_2\text{P}(\text{CH}_2)_n\text{PPh}_2]$ becomes slower as the chelate ring size increases (n increases).

Introduction

Transition-metal complexes with hydrotris(pyrazolyl)borato ligands (Tp^{R}) have been studied extensively.¹ In the field of organometallic chemistry, comparative studies with the corresponding $(\eta^5\text{-C}_5\text{R}_5)\text{M}$ systems have been carried out and, in the field of coordination chemistry, the Tp^{R} ligands have been regarded as versatile tripodal $\kappa^3\text{-N}_3$ donors along with 1,4,7-triazacyclononane derivatives. Although Tp^{R} complexes of many metals have been prepared, the syntheses can be quite challenging.

$\text{Tp}^{\text{R}}\text{RhL}_2$ complexes are usually prepared by treatment of RhClL_3 or $[\text{RhL}_2\text{Cl}]_2$ with the Tp^{R} anion.² Recently, Hill and co-workers reported a versatile Rh(I) precursor, $\text{TpRh}(\text{PPh}_3)_2$, bearing the nonsubstituted Tp ligand, which was obtained from $\text{RhCl}(\text{PPh}_3)_3$.³ The complex was found to be labile enough to lose one of the two PPh_3 ligands and was converted to a variety of adducts such as O_2 , alkene, alkyne, and thioacyl complexes via ligand replacement reactions and oxidative addition reactions. Prior to the present study, we also attempted a similar reaction using KTp^{iPr} . However, a complicated mixture was obtained and we obtained no evidence for formation of the corresponding product. As for $[\text{RhL}_2\text{Cl}]_2$ -type precursors, complexes having $\text{L}_2 =$ diene, $(\text{CH}_2=\text{CH}_2)_2$, dppe, and $(\text{CO})_2$ are easily prepared, but other derivatives can be difficult to obtain. For example, diphosphine complexes other than dppe derivative are not obtained in good yields. An alternative

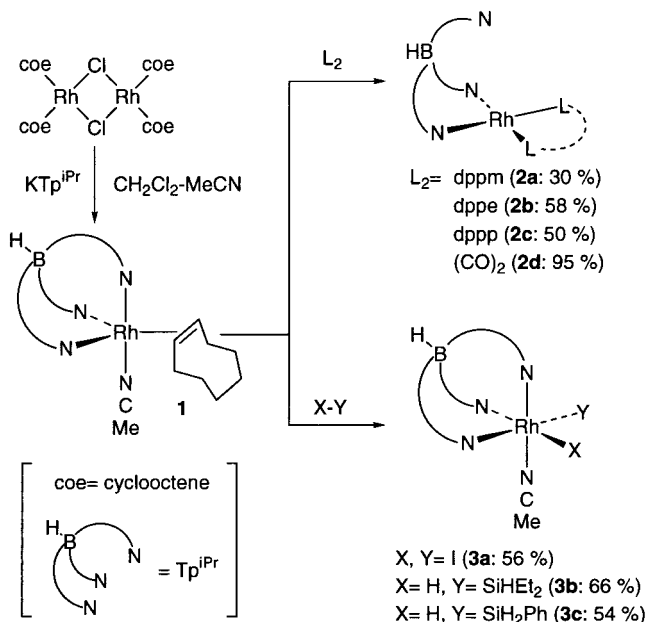
route to $\text{Tp}^{\text{R}}\text{RhL}_2$ is via ligand substitution in $\text{Tp}^{\text{R}}\text{RhL}'_2$, where L' is an easily dissociated ligand. Diene complexes, $\text{Tp}^{\text{R}}\text{Rh}(\text{diene})$,^{2a-f} are readily available but ligand substitution turns out to be not efficient. Thus, reaction

(2) Diene complexes: (a) Cocivera, M.; Desmond, T. J.; Ferguson, G.; Kaitner, B.; Lalor, F. J.; O'Sullivan, D. J. *Organometallics* **1982**, *1*, 1125. (b) Cocivera, M.; Ferguson, G.; Kaitner, B.; Lalor, F. J.; O'Sullivan, D. J.; Parvez, M.; Ruhl, B. *Organometallics* **1982**, *1*, 1132. (c) Cocivera, M.; Ferguson, G.; Lalor, F. J.; Szczecinski, P. *Organometallics* **1982**, *1*, 1139. (d) Bucher, U. E.; Currao, A.; Nesper, R.; Rügger, H.; Venanzi, L. M.; Younger, E. *Inorg. Chem.* **1995**, *34*, 66. (e) Bucher, U. E.; Fässler, T. F.; Hunziker, M.; Nesper, R.; Rügger, H.; Venanzi, L. M. *Gazz. Chim. Ital.* **1995**, *125*, 181. (f) Sanz, D.; Santa Maria, M. D.; Claramunt, R. M.; Cano, M.; Heras, J. V.; Campo, J. A.; Ruiz, F. A.; Pinilla, E.; Monge, A. *J. Organomet. Chem.* **1996**, *526*, 341. CO and isonitrile complexes: (g) Trofimenko, S. *Inorg. Chem.* **1971**, *10*, 1372. (h) Ghosh, C. K.; Graham, W. A. G. *J. Am. Chem. Soc.* **1987**, *109*, 4726. (i) Ghosh, C. K.; Graham, W. A. G. *J. Am. Chem. Soc.* **1989**, *111*, 375. (j) Jones, W. D.; Hessel, E. T. *Inorg. Chem.* **1991**, *30*, 778. (k) Hessel, E. T.; Jones, W. D. *Organometallics* **1992**, *11*, 1496. (l) Jones, W. D.; Hessel, E. T. *J. Am. Chem. Soc.* **1992**, *114*, 6087. (m) Jones, W. D.; Hessel, E. T. *J. Am. Chem. Soc.* **1993**, *115*, 554. (n) Rheingold, A. L.; Ostrander, R. L.; Haggerty, B. S.; Trofimenko, S. *Inorg. Chem.* **1993**, *32*, 3666. (o) Keyes, M. C.; Young, V. G., Jr.; Tolman, W. B. *Organometallics* **1996**, *15*, 4133. (p) Chauby, V.; Le Berre, S.; Daran, J.-C.; Commenges, G. *Inorg. Chem.* **1996**, *35*, 6345. (q) Connolly, N. G.; Emslie, D. J. H.; Metz, B.; Orpen, A. G.; Quayle, M. J. *J. Chem. Soc., Chem. Commun.* **1996**, 2289. (r) Purwoko, A. A.; Lees, A. J. *Inorg. Chem.* **1996**, *35*, 675. (s) Dhosh, C. K.; Rodgers, D. P. S.; Graham, W. A. G. *J. Chem. Soc., Chem. Commun.* **1988**, 1511. (t) Northcutt, T. O.; Lachicotte, R. J.; Jones, W. D. *Organometallics* **1998**, *17*, 5148. (u) Wick, D. D.; Northcutt, T. O.; Lachiotte, R. J.; Jones, W. D. *Organometallics* **1998**, *17*, 4484. Olefin complexes: (v) Trofimenko, S. *J. Am. Chem. Soc.* **1969**, *91*, 588. (w) Oldham, W. J.; Heinekey, D. M. *Organometallics* **1997**, *16*, 467. (x) Pérez, P. J.; Poveda, M. L.; Carmona, E. *Angew. Chem., Int. Ed. in Engl.* **1995**, *34*, 66. Rh(III) and polyhydride complexes: (y) May, S.; Reissal, P.; Powell, J. *Inorg. Chem.* **1980**, *19*, 1582. (z) Bucher, U. E.; Lengweiler, D.; von Philipsborn, W.; Venanzi, L. M. *Angew. Chem., Int. Ed. Engl.* **1990**, *29*, 548. (aa) Eckert, J.; Albinati, A.; Bucher, U. E.; Venanzi, L. M. *Inorg. Chem.* **1996**, *35*, 1292.

(3) Hill, A. F.; White, A. J. P.; Williams, D. J.; Wilton-Ely, J. D. E. *T. Organometallics* **1998**, *17*, 3152.

(1) (a) Trofimenko, S. *Chem. Rev.* **1993**, *93*, 943. (b) Kitajima, N.; Tolman, W. B. *Prog. Inorg. Chem.* **1995**, *43*, 419. (c) Kitajima, N.; Moro-oka, Y. *Chem. Rev.* **1994**, *94*, 737.

Scheme 1



of $Tp^{iPr}Rh(cod)$ with dppp in refluxing toluene (for 8 h) afforded only a trace amount of $Tp^{iPr}Rh(dppp)$. Bis(olefin) complexes are known to be much more labile than diene complexes and, as was expected, the bis(ethylene) complexes $Tp^R Rh(CH_2=CH_2)_2$ were found to readily react with 2e donors. However, this reaction usually results in monosubstitution to give the mixed-ligand complex $Tp^R Rh(CH_2=CH_2)(L)$.⁴ In addition, C–H activation of the ethylene ligand leading to the formation of vinyl complexes was often noted.⁵

During the course of our synthetic study on transition-metal–dioxygen complexes supported by the Tp^{iPr} ligand,^{6,7} we needed to synthesize $Tp^{iPr}Rh(L)_2$ type complexes. The attempted synthesis of $Tp^{iPr}Rh(coe)_2$ (coe = cyclooctene) as a precursor led instead to the isolation of the labile complex $Tp^{iPr}Rh(coe)(MeCN)$ (**1**). It was

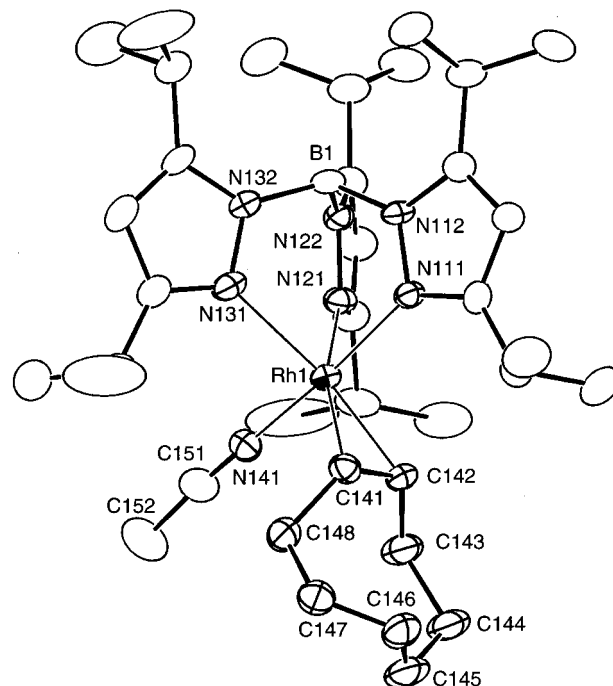


Figure 1. Molecular structure of **1** (one of the two independent molecules) drawn at the 30% probability level.

found that complex **1** serves as a versatile precursor for Rh(I) and Rh(III) species via ligand substitution and oxidative addition reactions, respectively.³

Results and Discussion

Synthesis of $Tp^{iPr}Rh(coe)(MeCN)$ (1**).** Attempted synthesis of the bis(coe) complex $Tp^{iPr}Rh(coe)_2$ by treatment of $[Rh(coe)_2Cl]_2$ with KTp^{iPr} in CH_2Cl_2 gave a mixture of products, from which neither the desired compound nor any characterizable product could be isolated. Changing the solvent to a CH_2Cl_2 –MeCN mixed system led to the isolation of product **1**, formulated as $Tp^{iPr}Rh(coe)(MeCN)$ (Scheme 1). Complex **1** decomposes under vacuum via dissociation of the coe ligand and must be stored at low temperature.

NMR data for **1** indicated the presence of Tp^{iPr} , coe, and MeCN ligands in a 1:1:1 ratio, and mirror-symmetrical structure was indicated by the pz ring proton signals appearing in a 1:2 ratio (Table 1). IR data implied κ^3 -coordination of the Tp^{iPr} ligand,^{6a} suggesting a mirror-symmetrical trigonal-bipyramidal structure, which was confirmed by X-ray crystallography. The molecular structure of **1** and selected structural parameters are shown in Figure 1 and Table 2, respectively. The unit cell of **1** contains two independent molecules with essentially the same geometry. The Tp^{iPr} ligand is coordinated to the Rh center in a κ^3 -fashion, and the overall structure can be described as trigonal-bipyramidal with a linear N111–Rh1–N141 (N211–Rh2–N241) axis and the two distinct Rh–N distances (Rh1–N111, Rh2–N211 (~ 2.1 Å: Rh–axial N) vs Rh1–N121, Rh1–N131, Rh2–N221, Rh2–N231 (> 2.2 Å: Rh–equatorial N)). The structural parameters of **1**, including the Rh–C (~ 2.08 Å) and C=C distances (1.43–1.45 Å), are comparable to those of the trigonal-bipyramidal diene complex (κ^3 - Tp^{iPr})Rh(η^4 -norbornadiene) (Rh–C, ~ 2.14 Å; C=C, 1.36–1.45 Å), previously reported by our

(4) (a) Oldham, W. J., Jr.; Heinekey, D. M. *Organometallics* **1997**, *16*, 467. (b) See ref 2x.

(5) Pérez, P. J.; Poveda, M. L.; Carmona, E. *Angew. Chem., Int. Ed. Engl.* **1995**, *34*, 231. See also: Gutiérrez-Puebla, E.; Monge, A.; Nicasio, M. N.; Pérez, P. J.; Poveda, M. L.; Carmona, E. *Chem. Eur. J.* **1998**, *4*, 2225.

(6) Cf. our recent works based on Tp^R systems. Rh–diene: (a) Akita, M.; Ohta, K.; Takahashi, Y.; Hikichi, S.; Moro-oka, Y. *Organometallics* **1997**, *16*, 4121. Ru–aqua: (b) Takahashi, Y.; Akita, M.; Hikichi, S.; Moro-oka, Y. *Inorg. Chem.* **1998**, *37*, 3186. Ru–diene: (c) Takahashi, Y.; Akita, M.; Hikichi, S.; Moro-oka, Y. *Organometallics* **1998**, *17*, 4884. Pd–OOR: (d) Akita, M.; Miyaji, T.; Hikichi, S.; Moro-oka, Y. *J. Chem. Soc., Chem. Commun.*, **1998**, 1005. Co–OOR: (e) Hikichi, S.; Komatsuzaki, H.; Kitajima, N.; Akita, M.; Mukai, M.; Kitagawa, T.; Moro-oka, Y. *Inorg. Chem.* **1997**, *36*, 266. (f) Hikichi, S.; Komatsuzaki, H.; Akita, M.; Moro-oka, Y. *J. Am. Chem. Soc.* **1998**, *120*, 4699. Co–, Ni–oxo: (g) Hikichi, S.; Yoshizawa, M.; Sasakura, Y.; Akita, M.; Moro-oka, Y. *J. Am. Chem. Soc.* **1998**, *120*, 10567. Fe–, Co–, Ni–alkyl: (h) Akita, M.; Shirasawa, N.; Hikichi, S.; Moro-oka, Y. *Chem. Commun.* **1998**, 973. (i) Shirasawa, N.; Akita, M.; Hikichi, S.; Moro-oka, Y. *Chem. Commun.* **1999**, 417. Fe–catecholate: (j) Ogihara, T.; Hikichi, S.; Akita, M.; Moro-oka, Y. *Inorg. Chem.*, **1998**, *37*, 2614. Mn–OO(R): (k) Komatsuzaki, H.; Nagasu, Y.; Suzuki, K.; Shibasaki, T.; Satoh, M.; Ebina, F.; Hikichi, S.; Akita, M.; Moro-oka, Y. *J. Chem. Soc., Dalton Trans.* **1998**, 511. (l) Komatsuzaki, H.; Ichikawa, S.; Hikichi, S.; Akita, M.; Moro-oka, Y. *Inorg. Chem.* **1998**, *37*, 3652. (m) Komatsuzaki, H.; Sakamoto, N.; Satoh, M.; Hikichi, S.; Akita, M.; Moro-oka, Y. *Inorg. Chem.* **1998**, *37*, 6554. A short review: (n) Akita, M.; Fujisawa, K.; Hikichi, S.; Moro-oka, Y. *Res. Chem. Intermed.* **1998**, *24*, 291.

(7) Abbreviations used in this paper: Tp^{iPr} = hydridotris(3,5-diisopropylpyrazolyl)borate; Tp^H = hydridotris(pyrazolyl)borate; Tp^{Me} = hydridotris(3,5-dimethylpyrazolyl)borate; Tp^R = substituted Tp derivatives; pz = pyrazolyl group; coe = cyclooctene.

Table 1. NMR and IR Data for $\text{Tp}^{\text{iPr}}\text{Rh}(\text{coe})(\text{MeCN})$ (**1**), $\text{Tp}^{\text{iPr}}\text{RhL}_2$ (**2**), and $\text{Tp}^{\text{iPr}}\text{Rh}(\text{X})(\text{Y})(\text{MeCN})$ (**3**)^a

complex	³¹ P, ¹³ C NMR L	¹ H NMR				IR ^d ν(B-H)
		L, X, Y, MeCN	pz-H	CHMe ₂ ^b	CHMe ₂ ^c	
1 ^{e,f} (coe, MeCN)	38.1 (d, 18, ^g =CH) ^g	4.13–4.11 (2H, m, =CH), 0.61 (3H, s, MeCN)	6.17 (2H), 5.68 (1H)	3.86 (2H), 3.60 (1H), 3.43 (1H)	1.72 (6H), 1.48 (6H), 1.31 (6H), 1.26 (6H), 1.22 (6H), 1.17 (6H)	2544
2a ^e (dppm)	19.5 (d, 155) ^h		5.95 (3H)	3.68 (3H), 3.12 (3H)	1.23 (18H), 1.07 (18H)	2488
2b ^j (dppe)	63.4 (d, 183) ^h	7.67 (brs, 8H, Ph), 7.01 (m, 12H, Ph), 7.01 (m, 12H, Ph)	5.74 (3H)	3.52 (3H), 3.07 (3H)	1.18 (18H), 1.04 (18H)	2486
2c ^j (dppp)	27.5 (dd, 164, ^h 29) ^h	7.74 (m, 4H, Ph), 7.17–6.82 (m, 16H, Ph), 2.16 (m, 6H, (CH ₂) ₃)	6.05 (1H), 5.29 (2H)	3.47 (2H), 3.38 (1H), 3.13 (1H), 2.68 (2H)	1.47 (3H), 1.32 (3H), 1.20 (3H), 1.13 (3H), 1.0 (3H), 0.20 (3H)	2488
2d ^j (CO) ₂	190.3 ^k (d, 69.8) ^g		5.83 (3H)	3.41 (3H), 3.34 (3H)	1.26 (18H), 1.20 (18H)	2547, 2044, ^l 1966 ^l
3a ^j (I, I)		1.18 (3H, s)	6.08 (1H), 6.01 (2H)	5.34 (1H), 4.60 (2H), 3.45 (3H)	1.59 (6H), 1.57 (6H), 1.05 (6H), 1.01 (12H)	2554
3b ^e (H, SiH _{Et} ₂)		4.56 (1H, s, SiH), 0.82 (3H, s, MeCN), –16.40 (1H, d, 19.3, RhH)	6.14 (1H), 5.97 (1H), 5.88 (1H)	4.01 (1H), 3.82–3.69 (3H), 3.60 (3H), 3.55 (3H)	1.52 (3H), 1.45 (3H), 1.40–0.99 (40H) ^m	2551, 2055 ⁿ
3c ^{e,o} (H, SiH ₂ Ph)		5.35, 5.13 (1H × 2, d, 4.8, SiH ₂), 0.66 (3H, s, MeCN), –15.30 (1H, d, 18.2, RhH)	6.11 (1H), 6.02 (1H), 5.74 (1H)	4.00–3.53 (6H)	1.47 (3H), 1.37 (3H), 1.28 (3H), 1.24 (3H), 1.23 (3H), 1.18 (3H), 1.164 (3H), 1.157 (3H), 1.150 (3H), 1.14 (3H), 1.04 (3H), 1.01 (3H)	2544, 2066 ⁿ

^a δ values are given in ppm; the multiplicity and coupling constant (in Hz) are shown in parentheses. ^b Septet ($J \approx 7$ Hz) or multiplet signals. ^c Doublet signals ($J \approx 7$ Hz). ^d In cm^{-1} , measured as KBr pellets. ^e NMR spectra were observed in C_6D_6 . ^f The other signals: δ_H 2.62–2.59 (2H, m), 2.16–1.91 (8H, m), 1.72 (2H, br); δ_C 164.9, 160.5, 155.7, 154.8 (pz), 121.8 (d, $J_{\text{Rh-C}} = 17.5$ Hz, MeCN), 100.3, 97.2 (pz), 29.9, 28.1, 27.8, 27.4, 26.6, 25.2, 24.8, 24.6, 23.8, 23.7, 23.4 (iPr), 2.3 (MeCN). ^g $J_{\text{Rh-C}}$. ^h $J_{\text{Rh-P}}$. ⁱ $J_{\text{P-P}}$. ^j NMR spectra were observed in CDCl_3 . ^k The other signals: δ_C 160.0, 155.7, 97.6 (pz), 29.0, 26.3, 23.5, 23.4 (iPr). ^l ν(C≡O). ^m Broad and overlapped with the Et signals. ⁿ ν(Rh–H). ^o Ph signals: δ_H 7.68–7.63 (2H, m, Ph), 7.12–7.08 (3H, m, Ph).

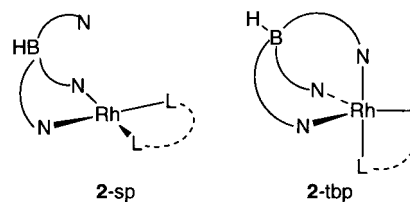
Table 2. Selected Structural Parameters for **1**^a

molecule 1		molecule 2	
Rh1–N111	2.109(5)	Rh2–N211	2.107(6)
Rh1–N121	2.258(6)	Rh2–N221	2.218(5)
Rh1–N131	2.215(6)	Rh2–N231	2.289(6)
Rh1–N141	1.968(6)	Rh2–N241	1.979(5)
Rh1–C141	2.066(7)	Rh2–C241	2.077(7)
Rh1–C142	2.086(7)	Rh2–C242	2.087(7)
C141–C142	1.45(1)	C241–C242	1.438(9)
N111–Rh1–N121	86.8(2)	N211–Rh2–N221	87.2(2)
N111–Rh1–N131	86.3(2)	N211–Rh2–N231	86.8(2)
N111–Rh1–N141	175.6(2)	N211–Rh2–N241	175.6(2)
N111–Rh1–C141	94.5(2)	N211–Rh2–C241	93.3(3)
N111–Rh1–C142	93.8(2)	N211–Rh2–C242	93.6(3)
N121–Rh1–N131	83.5(2)	N221–Rh2–N231	84.0(2)
N121–Rh1–N141	89.2(2)	N221–Rh2–N241	90.7(2)
N121–Rh1–C141	159.7(2)	N221–Rh2–C241	156.9(2)
N121–Rh1–C142	118.8(2)	N221–Rh2–C242	116.5(2)
N131–Rh1–N141	91.4(2)	N231–Rh2–N241	89.1(2)
N131–Rh1–C141	116.8(3)	N231–Rh2–C241	119.1(2)
N131–Rh1–C142	157.7(2)	N231–Rh2–C242	159.5(2)
N141–Rh1–C141	89.9(3)	N241–Rh2–C241	90.2(2)
N141–Rh1–C142	89.8(3)	N241–Rh2–C242	90.8(3)
C141–Rh1–C142	40.9(3)	C241–Rh2–C242	40.4(2)

^a Interatomic distances in Å and bond angles in deg.

group.^{6a} NMR and IR data indicate that the five-coordinate structure is retained in solution.

Ligand Substitution Reactions of 1 Leading to $\text{Tp}^{\text{iPr}}\text{Rh}(\text{L})_2$ (2**). (i) Diphosphine Complexes **2a**–**c**.**

Chart 1

Addition of diphosphines or CO to **1** resulted in substitution reactions to give the square-planar complexes **2a**–**d** in a selective manner. The dppe complex **2b** could be also synthesized by an alternative route, namely the reaction of $[\text{RhCl}(\text{dppe})_2]$ with KTp^{iPr} in refluxing acetone.

The composition of the substituted products, $\text{Tp}^{\text{iPr}}\text{RhL}_2$, and loss of the coe and MeCN ligands were readily confirmed by NMR data (Table 1). As for the coordination geometry of the $\text{Tp}^{\text{R}}\text{RhL}_2$ -type complexes, previous studies² have established that (1) κ^2 - and κ^3 -coordination of the Tp^{R} ligand leads to four-coordinated square-planar structures and five-coordinated trigonal-bipyramidal structures, respectively, and (2) in a solution, the two isomeric structures are interconverted. This dynamic behavior often results in averaging of the three pz^{R} NMR signals. Coordination of the free pz^{R} group in **2-sp** (Chart 1) leads to a tbp structure (**2-tbp**), and dissociation of either of the equatorial pz^{R} groups would

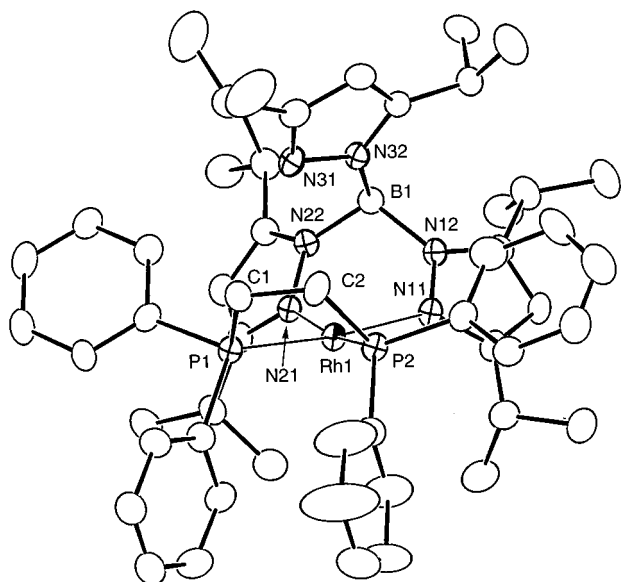


Figure 2. Molecular structure of **2b** drawn at the 30% probability level.

Table 3. Selected Structural Parameters for $\text{Tp}^{\text{iPr}}\text{Rh}(\text{L}_2)$ (**2**)^a

complex (L_2)	2a (dppm)	2b (dppe)	2c (dppp)
Rh1–P1	2.210(1)	2.226(2)	2.228(1)
Rh1–P2	2.2150(8)	2.205(2)	2.219(1)
Rh1–N11	2.106(3)	2.095(6)	2.086(4)
Rh1–N21	2.140(2)	2.099(5)	2.120(4)
Rh1...N31	3.081(3)	3.419(7)	3.381(5)
P1–C1	1.842(3)	1.863(9)	1.842(7)
P2–C(<i>n</i>) ^b	1.853(4)	1.83(1)	1.832(8)
P1–Rh1–P2	73.12(4)	80.90(6)	88.17(5)
P1–Rh1–N11	174.68(6)	173.1(2)	176.0(1)
P1–Rh1–N21	102.16(9)	96.5(2)	95.4(1)
P2–Rh1–N11	102.56(7)	98.2(1)	93.7(1)
P2–Rh1–N21	172.49(7)	169.5(2)	169.2(1)
N11–Rh1–N21	82.5(1)	83.2(2)	82.1(2)

^a Interatomic distances in Å and bond angles in deg. ^b P2–CH₂.

lead to an isomeric square-planar structure. When the interconversion occurs at a rate faster than the NMR coalescence time scale, the three pz^R signals would be observed as a single set of resonances.

The molecular structures of **2a–c** were determined by X-ray crystallography. An ORTEP view of **2b** is shown in Figure 2 and the selected structural parameters of **2a–c** are compared in Table 3. ORTEP views of **2a,c** are included in the Supporting Information, and their numbering systems are the same as that of **2a** with the exception of the P–(CH₂)_{*n*}–P parts (P1–C1–P2 (**2a**); P1–C1–C2–C3–P2 (**2c**)). The diphosphine complexes **2a–c** adopt similar square-planar geometries with a $\kappa^2\text{-Tp}^{\text{iPr}}$ ligand, as can be seen from the Rh1...N31 separations out of the bonding interaction. The κ^2 -coordination is also supported by the ν_{BH} values appearing below 2500 cm⁻¹.^{6a} The noncoordinated pz^{iPr} rings are laid almost parallel to the P₂N₂–Rh coordination plane so as to reduce the steric repulsion among the isopropyl groups. The P1–Rh1–P2 bite angle increases as the (CH₂)_{*n*} bridge becomes longer, but the other parameters, including the N11–Rh1–N21 bite angles, are not much affected by the bridge length (*n*).

¹H NMR spectra of **2a–c** depend considerably on *n*. The symmetry of the structure can be predicted from

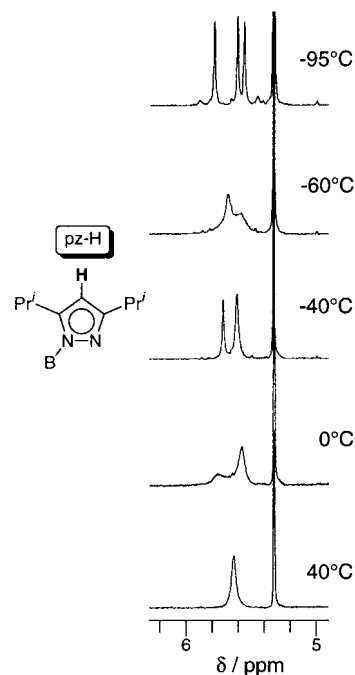


Figure 3. Variable-temperature ¹H NMR spectra of **2b** observed in CD₂Cl₂ at 400 MHz.

the pattern of the CH signals of the 4-position of the pyrazolyl ring (pz-H). The dppp complex **2c** gives, at room temperature, a spectrum containing two pz-H signals in a 1:2 ratio. Taking into account the equivalent ³¹P NMR signals, the NMR features are consistent with the C_s-symmetrical square-planar geometry confirmed by X-ray crystallography (**2-sp** in Chart 1). In contrast to **2c**, the dppe complex **2a** gives a single sharp pz-H signal at room temperature, indicating dynamic behavior as discussed above. X-ray and IR results (see above) suggest that the square-planar geometry is the ground-state structure. The pz-H signal remains as a singlet down to –60 °C and separates into two singlets in a 1:2 ratio at –95 °C. The pattern at –95 °C is similar to that of **2c** discussed above and suggest that the $\kappa^2\text{-}\kappa^3$ interconversion is frozen out at a low temperature. Behavior of the dppe complex **2b** is between that of **2a** and **2c** (Figure 3). For example, the broad singlet pz-H signal observed at room temperature sharpens at 110 °C (in toluene-*d*₈) and separates into two singlet signals in a 1:2 ratio below 0 °C (in CD₂Cl₂). Because lowering the temperature below –60 °C causes separation into three pz-H signals, the rotation around the B–N axis in the noncoordinated B–pz^{iPr} moiety is fixed at a very low temperature. These spectral features reveal that (1) as the P–Rh–P bite angle becomes acute (as *n* decreases), the interconversion between the square-planar (**2-sp**) and trigonal-bipyramidal structure (**2-tbp**) becomes faster and (2) in the ground-state structure, the diphosphine complex **2** adopts the square-planar geometry as revealed by the X-ray and IR data ($\nu_{\text{BH}} < 2500$ cm⁻¹).^{6a}

The dependence of the $\kappa^2\text{-}\kappa^3$ interconversion rate on *n* can be interpreted in terms of bulkiness of the diphosphine ligands. A bulky ligand should favor the less sterically congested four-coordinate sp form (**2-sp**) over the five-coordinate tbp form (**2-tbp**). The steric bulkiness of the ligands can be estimated by the P–Rh–P bite angles: 73.12(4)° (dppm) < 80.90(6)°

(dppe) < 88.17(5)° (dppp). The dppp complex **2c** would suffer much steric hindrance in the tbp structure due to the repulsion among the Tp^{iPr} substituents and the phenyl groups. As the $(\text{CH}_2)_n$ bridge becomes shorter, the repulsion may become less serious, facilitating the dynamic behavior by way of the congested tbp structure; nevertheless the ground-state structure is the sp form.

To our surprise, we could not find a linear relationship between the P–Rh–P bite angle and the ^{31}P NMR parameters (δ_{P} and $J_{\text{Rh-P}}$ values) or a significant dependence of the δ_{P} and $J_{\text{Rh-P}}$ values on the measurement temperatures in the range of room temperature to -95°C (e.g. **2a**: δ_{P} 4.9–5.4; $J_{\text{Rh-P}}$ = 151–156 Hz).

(ii) Dicarboxyl Complex 2d. Behavior of the dicarbonyl complex **2d** is considerably different from that of the diphosphine complexes **2a–c**. The ν_{BH} vibration appearing higher than 2500 cm^{-1} indicates κ^3 -coordination of the Tp^{iPr} ligand, and the single pz-H signal (^1H NMR) suggests occurrence of fast κ^2 – κ^3 interconversion. Although these data appear to be consistent with the trigonal-bipyramidal structure as observed for **2a**, preliminary X-ray crystallography revealed a distorted-square-pyramidal geometry for **2d**.⁸ The five-coordinate structure including the κ^3 - Tp^{iPr} ligand should be a result of the Lewis acidic rhodium center caused by the electron-withdrawing carbonyl ligands.

Oxidative Addition to 1 Leading to $\text{Tp}^{\text{iPr}}\text{Rh}(\text{X})(\text{Y})(\text{MeCN})$ (3). Treatment of **1** with I_2 in CH_2Cl_2 gave the red adduct **3a**. The ν_{BH} vibration at 2554 cm^{-1} suggests κ^3 -coordination of the Tp^{iPr} ligand,^{6a} and a ^1H NMR spectrum indicated a mirror-symmetrical structure and loss of the coe ligand. These spectroscopic features led to the assignment of **3a** as an octahedral complex, $\text{Tp}^{\text{iPr}}\text{RhI}_2(\text{MeCN})$, which resulted from oxidative addition of I_2 . $\text{Tp}^{\text{H}}\text{Rh}(\text{X})(\text{Y})(\text{L})$ - and $\text{Tp}^{\text{Me}}\text{Rh}(\text{X})(\text{Y})(\text{L})$ -type Rh(III) complexes⁷ obtained from $\text{RhCl}_3\cdot 3\text{H}_2\text{O}$ were extensively studied by Powell,⁹ who also reported the related dichloro complexes $\text{Tp}^{\text{H}}\text{RhCl}_2(\text{MeCN})$ and $\text{Tp}^{\text{Me}}\text{RhCl}_2(\text{MeCN})$.

Reaction of **1** with hydrosilanes also resulted in Si–H oxidative addition. The reaction with di- (H_2SiEt_2) and trihydrosilane (H_3SiPh) readily afforded octahedral silyl–hydrido complexes, $\text{Tp}^{\text{iPr}}\text{Rh}(\text{H})(\text{SiR}_3)(\text{MeCN})$ (**3b,c**, respectively), but monohydrosilane (HSiEt_3) left **1** unreacted, presumably due to the steric congestion around the Si–H moiety. Assignment of complexes **3b,c** was based on (i) the ν_{BH} value ($> 2500\text{ cm}^{-1}$),^{6a} (ii) the Rh–H signals ($\delta_{\text{H}}(\text{Rh-H})$ and ν_{RH}), and (iii) the presence of the MeCN ligand. In the case of **3c**, the three pz rings and the SiH_2 hydrogen atoms were inequivalent due to the chiral Rh center.

It is notable that, in the oxidative addition reactions of **1**, the coe ligand rather than the MeCN ligand is removed during the reaction. This is presumably owing to the decreased back-donation ability of the Rh(III) center to the coe ligand, and the Lewis acidic Rh(III) center should be stabilized by a σ -donor such as MeCN.

Attempted reaction of **1** with H_2 and O_2 afforded a complicated mixture similar to that obtained when **1** was exposed to reduced pressure.

Concluding Remarks. The Rh(I) species $\text{Tp}^{\text{iPr}}\text{Rh}(\text{coe})(\text{MeCN})$ (**1**) is labile enough to undergo ligand substitution with 2e donors (L) to give $\text{Tp}^{\text{iPr}}\text{Rh}(\text{L})_2$ -type Rh(I) complexes, which are hardly obtained from other precursors such as diene, bis(ethylene), and carbonyl complexes. Complex **1** is also susceptible to oxidative addition to give the Rh(III) species $\text{Tp}^{\text{iPr}}\text{Rh}(\text{X})(\text{Y})(\text{MeCN})$. Thus, complex **1** serves as a versatile precursor for $\text{Tp}^{\text{iPr}}\text{Rh}^{\text{I,III}}$ complexes.

In this study we examined only the Tp^{iPr} system, but analogous $\text{Tp}^{\text{R}}\text{Rh}(\text{coe})(\text{MeCN})$ complexes should be accessible via a similar procedure. Actually, Ozawa and co-workers prepared the 3,5-dimethylpyrazolyl derivative of **1** following our procedure and examined the synthesis of π -allyl complexes.¹⁰

It is also noted that the κ^2 – κ^3 interconversion rate of the diphosphine complexes $\text{Tp}^{\text{iPr}}\text{Rh}[\text{Ph}_2\text{P}(\text{CH}_2)_n\text{PPh}_2]$ (**2a–c**) is dependent on the chelate ring size; e.g. as the chelate ring size increases (n increases), the interconversion becomes slower.

Experimental Section

General Methods. All manipulations were carried out under an inert atmosphere by using standard Schlenk tube techniques. Ether (Na–K alloy), toluene (Na), CH_2Cl_2 ($\text{P}_{4}\text{O}_{10}$), acetone (KMnO_4 –molecular sieves), and MeCN (CaH_2) were treated with appropriate drying agents, distilled, and stored under argon. ^1H and ^{13}C NMR spectra were recorded on a JEOL EX400 (^1H , 400 MHz) spectrometer. Solvents for NMR measurements containing 0.5% TMS were dried over molecular sieves, degassed, distilled under reduced pressure, and stored under Ar. IR and FD-MS spectra were obtained on a JASCO FT/IR 5300 spectrometer and a Hitachi M80 mass spectrometer, respectively. KTp^{iPr} ,¹¹ $[\text{RhCl}(\text{coe})_2]_2$,¹² and $[\text{RhCl}(\text{dppe})_2]_2$ ¹³ were prepared according to the reported method. Other chemicals were purchased and used as received.

Preparation of $\text{Tp}^{\text{iPr}}\text{Rh}(\text{coe})(\text{MeCN})$ (1). KTp^{iPr} (1.13 g, 2.24 mmol) was added to $[\text{RhCl}(\text{coe})_2]_2$ (799 mg, 1.11 mmol) suspended in CH_2Cl_2 (30 mL) and MeCN (5 mL), and the resultant mixture was stirred for 10 min at room temperature. After filtration through a Celite pad followed by concentration, the product **1**·2MeCN (1.42 g, 1.78 mmol, 80% yield) was obtained as red prisms by cooling at -20°C . Complex **1** must be dried under a slow Ar stream and decomposed when dried under reduced pressure. The amount of the MeCN solvate included in a sample was measured by ^1H NMR and used as it was. Satisfactory elemental analysis results were not obtained despite several attempts, due to decomposition during the drying process under reduced pressure.

Preparation of $\text{Tp}^{\text{iPr}}\text{Rh}(\text{dppm})$ (2a). When a mixture of **1**·10MeCN (552.4 mg, 0.489 mmol) and dppm (185.5 mg, 0.483 mmol) dissolved in CH_2Cl_2 (10 mL), the solution color changed from orange to deep red. After this mixture was stirred for 2 h, the volatiles were evaporated under reduced pressure. Crystallization of the residue from toluene–MeOH gave deep red crystals of **2a** (139.6 mg, 0.147 mmol, 30% yield). Anal. Calcd for $\text{C}_{54}\text{H}_{76}\text{BN}_6\text{O}_2\text{P}_2\text{Rh}$ (**2a**·2MeOH): C, 63.78; H, 7.53; N, 8.26. Found: C, 63.80; H, 7.91; N, 8.65.

Preparation of $\text{Tp}^{\text{iPr}}\text{Rh}(\text{dppe})$ (2b). (i) From 1. A mixture of **1**·15MeCN (201.5 mg, 0.151 mmol) and dppe (61.4

(8) Because the single crystal decomposed during the data collection, details of the crystallographic results are not reported herein. Cell parameters were as follows: $a = 9.956(2)\text{ \AA}$, $b = 16.531(8)\text{ \AA}$, $c = 19.414(6)\text{ \AA}$, $\beta = 97.63(2)^\circ$, $V = 3167(2)\text{ \AA}^3$, space group $P2_1/c$.

(9) May, S.; Reinsalu, P.; Powell, J. *Inorg. Chem.* **1980**, *19*, 1582.

(10) See footnote 6b in the following paper: Ikeda, S.; Maruyama, Y.; Ozawa, F. *Organometallics* **1998**, *17*, 3770.

(11) Kitajima, N.; Fujisawa, K.; Fujimoto, C.; Moro-oka, Y.; Hashimoto, S.; Kitagawa, T.; Toriumi, K.; Tatsumi, K.; Nakamura, A. *J. Am. Chem. Soc.* **1992**, *114*, 1277.

(12) van der Ent, A.; Onderdelinden, A. L. *Inorg. Synth.* **1990**, *28*, 90.

(13) Fairlie, D. P.; Bosnich, B. *Organometallics* **1988**, *7*, 936.

Table 4. Crystallographic Data

compd	1·3MeCN	2a	2b·1/2Et ₂ O	2c
formula	C ₄₃ H ₇₂ BN ₁₀ Rh	C ₅₂ H ₆₈ BN ₆ P ₂ Rh	C ₅₅ H ₇₅ BN ₆ O _{0.5} P ₂ Rh	C ₅₄ H ₇₂ BN ₆ P ₂ Rh
fw	842.83	952.81	1003.90	980.87
cryst syst	triclinic	monoclinic	monoclinic	monoclinic
space group	<i>P</i> 1	<i>P</i> 2 ₁ / <i>c</i>	<i>C</i> 2/ <i>c</i>	<i>P</i> 2 ₁
<i>a</i> /Å	18.568(7)	11.075(2)	44.554(8)	11.897(2)
<i>b</i> /Å	21.95(1)	37.925(3)	13.621(2)	18.76(1)
<i>c</i> /Å	12.552(2)	12.988(2)	18.563(2)	12.722(2)
α /deg	101.76(3)			
β /deg	93.71(2)	112.979(1)	108.77(2)	113.47(1)
γ /deg	100.88(4)			
<i>V</i> /Å ³	4889(3)	5023(1)	10666(3)	2605(2)
Z	4	4	8	2
<i>d</i> _{calcd} /g cm ⁻³	1.15	1.26	1.25	1.25
μ /cm ⁻¹	3.87	4.43	4.22	4.30
max 2 θ /deg	50.0	55.1	55.1	55.1
no. of unique data	17 168	10 281	8577	5529
no. of params refined	943	571	604	589
<i>R</i> 1	0.071 (9690 data)	0.071 (9850 data)	0.087 (7859 data)	0.045 (5469 data)
(for data with <i>F</i> > 4 σ (<i>F</i>))				
wR2 (for all data)	0.201	0.194	0.247	0.135

mg, 0.154 mmol) dissolved in CH₂Cl₂ (10 mL) was stirred for 5 h at room temperature. After removal of the volatiles under reduced pressure, the residue was washed with MeCN. Crystallization of the resultant yellow residue from Et₂O–MeCN gave **2b**·0.5Et₂O as yellow-orange crystals (112.1 mg, 0.112 mmol, 74% yield).

(ii) From [RhCl(dppe)]₂. An acetone solution (30 mL) of [RhCl(dppe)]₂ (500 mg, 0.467 mmol) and KTp^{iPr} (472.9 mg, 0.937 mmol) was refluxed for 3 h. After removal of the volatiles, the product was extracted with ether and filtered through Celite. Crystallization from Et₂O–MeCN gave **2c**·0.5Et₂O in 58% yield (540.4 mg, 0.538 mmol). Anal. Calcd for C₅₃H₇₀BN₆P₂Rh (**2c**): C, 65.84; H, 7.30; N, 8.69. Found: C, 65.93; H, 7.31; N, 8.42.

Preparation of Tp^{iPr}Rh(dppp) (2c). A mixture of **1**·10MeCN (604.3 mg, 0.535 mmol) and dppp (244.1 mg, 0.592 mmol) dissolved in CH₂Cl₂ (10 mL) was stirred for 3 h at room temperature. After removal of the volatiles under reduced pressure, the residue was washed with MeCN. Crystallization of the resultant yellow residue from CH₂Cl₂–MeCN gave **2c** as yellow crystals (259.7 mg, 0.265 mmol, 50% yield). Anal. Calcd for C_{54.5}H₇₃BN₆P₂ClRh (**2d**·0.5CH₂Cl₂): C, 63.97; H, 7.19; N, 8.21. Found: C, 63.99; H, 6.87; N, 8.56.

Preparation of Tp^{iPr}Rh(CO)₂ (2d). A CH₂Cl₂ solution (10 mL) of **1**·10MeCN (429.9 mg, 0.380 mmol) was stirred under CO atmosphere for 7.5 h at room temperature. After removal of the volatiles under reduced pressure, the residue was washed with MeOH. Crystallization from CH₂Cl₂–MeOH gave **2d** (225.3 mg, 0.361 mmol, 95% yield) as orange plates. Anal. Calcd for C_{29.2}H_{46.4}BN₆O₂Cl_{0.4}Rh (**2d**·0.2CH₂Cl₂): C, 54.68; H, 7.29; N, 13.10. Found: C, 54.17; H, 7.00; N, 13.28.

Preparation of Tp^{iPr}RhI₂(MeCN) (3a). To a CH₂Cl₂ solution (10 mL) of **1**·2MeCN (1.62 g, 2.03 mmol) was added I₂ (653.3 mg, 2.57 mmol), and the resulting mixture was stirred for 10 min at room temperature. Then the mixture was washed with saturated aqueous Na₂S₂O₃ solution, and the organic phase was dried over Na₂SO₄. Concentration followed by alumina column chromatography gave **3a** (983.1 mg, 1.14 mmol, 56% yield) as red solids. Anal. Calcd for C₂₉H₄₉BN₇I₂·Rh: C, 40.35; H, 5.72; N, 11.36. Found: C, 40.50; H, 5.95; N, 11.38.

Preparation of Tp^{iPr}Rh(H)(SiH₂Et₂)(MeCN) (3b). To a toluene solution (10 mL) of **1**·2MeCN (813 mg, 1.02 mmol) was added H₂SiEt₂ (160 μ L, 1.22 mmol) at room temperature, and the resulting mixture was stirred for 20 min. Removal of the volatiles under reduced pressure followed by crystallization from ether–hexane afforded **3b** (468 mg, 0.673 mmol, 66% yield) as colorless solids. Anal. Calcd for C₃₃H₆₁BN₇SiRh: C, 57.13; H, 8.83; N, 13.77. Found: C, 56.81; H, 8.81; N, 14.05.

Preparation of Tp^{iPr}Rh(H)(SiH₂Ph)(MeCN) (3c). To a toluene solution (10 mL) of **1**·2MeCN (428 mg, 0.536 mmol) was added H₃SiPh (0.22 mL, 1.79 mmol) at room temperature, and the resulting mixture was stirred for 20 min. Removal of the volatiles under reduced pressure followed by crystallization from octane afforded **3c** (208 mg, 0.289 mmol, 54% yield) as colorless solids. An analytically pure sample was not obtained despite several attempts.

X-ray Crystallography. Single crystals of **1** (MeCN), **2a** (toluene–MeOH), **2b** (ether–MeCN), and **2c** (CH₂Cl₂–MeCN) were obtained by recrystallization from the solvent systems shown in parentheses and mounted on glass fibers. The crystallographic data are summarized in Table 4.

Diffraction measurement of **1** was made on a Rigaku AFC5S automated four-circle diffractometer by using graphite-monochromated Mo K α radiation ($\lambda = 0.710 69$ Å) at -60 °C. The unit cell was determined and refined by a least-squares method using 20 independent reflections. Data were collected with an ω – 2θ scan technique. If $\sigma(F)/F$ was more than 0.1, a scan was repeated up to three times and the results were added to the first scan. Three standard reflections were monitored every 100 measurements. All data processing was performed on a FACOM A-70 computer. Neutral scattering factors were obtained from the standard source.¹⁴ In the reduction of data, Lorentz, polarization, and empirical absorption corrections (ψ scan) were made.

Diffraction measurements of **2a–c** were made on a Rigaku RAXIS IV imaging plate area detector with Mo K α radiation ($\lambda = 0.710 69$ Å). All the data collections were carried out at room temperature. Indexing was performed from three oscillation images which were exposed for 4 min. The crystal-to-detector distance was 110 mm. Data collection parameters were as follows: the oscillation range, 5° (**2a**), 3° (**2b**), 3.5° (**2c**); the number of oscillation images, 26 (**2a**), 30 (**2b**), 22 (**2c**); the exposed time, 40 min. Readout was performed with a pixel size of 100 μ m \times 100 μ m. Neutral scattering factors were obtained from the standard source.¹⁴ In the reduction of data, Lorentz, polarization, and empirical absorption corrections were made.¹⁵

The structures were solved by a combination of the direct methods (SHELXL 87 and DIRDIF). Least-squares refinements were carried out using SHELEXL93 linked to teXsan. All of the non-hydrogen atoms except for the MeCN solvates in **1**·3MeCN were refined anisotropically. The disordered coe ligand in molecule 2 of **1**·3MeCN was refined by taking into

(14) *International Tables for X-ray Crystallography*, Kynoch Press: Birmingham, U.K., 1975; Vol. 4.

(15) Stuart, D.; Walker, N. *Acta Crystallogr.* **1979**, *A35*, 925.

account the minor components, and the occupancy factors were C245–C246:C345–C346 = 0.63:0.37. The methyl hydrogen atoms, except those in the MeCN solvates (not located) in **1**·3MeCN, were refined using the riding models, and the other hydrogen atoms except for the disordered parts were fixed at the calculated positions and not refined.

Acknowledgment. We are grateful to the Ministry of Education, Science, Sports and Culture of the Japa-

nese Government for financial support of this research (Grant-in-Aid for Specially Promoted Scientific Research: 08102006).

Supporting Information Available: Tables listing crystallographic results and atomic numbering schemes. This material is available free of charge via the Internet at <http://pubs.acs.org>.

OM990104M